

Citation info:

Jonas Botterman, Koen Van den Eeckhout, Ives De Baere, Dirk Poelman,
Philippe F. Smet, "Mechanoluminescence in BaSi₂O₂N₂:Eu", Acta Materialia
60 (2012) 5494-5500

Mechanoluminescence in BaSi₂O₂N₂:Eu

Jonas Botterman^{1,2}, Koen Van den Eeckhout^{1,2}, Ives De Baere³, Dirk Poelman^{1,2}, Philippe F. Smet^{1,2,*}

¹ LumiLab, Dept. Solid State Sciences, Ghent University, Krijgslaan 281-S1, 9000 Gent, Belgium.

² Center for Nano- and Biophotonics (NB-Photonics), Ghent University, Belgium.

³ Department of Materials Science and Engineering, Ghent University, Technologiepark Zwijnaarde 903, 9052 Zwijnaarde, Belgium

*Corresponding author. Tel: +32 9 264 43 53; fax: +32 9 264 49 96

E-mail address: philippe.smet@ugent.be

Abstract: Mechanoluminescence (ML), a general term for the phenomenon in which light emission occurs during any mechanical action on a solid, can be divided roughly into two classes: destructive ML and non-destructive ML. For practical use in high-end applications (e.g. pressure sensors), materials with non-destructive ML properties are preferred. This paper reports on the strong non-destructive ML in BaSi₂O₂N₂:Eu. When irradiated in advance with UV or blue light, this phosphor shows intense blue-green light emission upon mechanical stimulation such as friction or pressure. The ML has an emission band peaking at 498 nm, which is about 4 nm red-shifted compared to the steady state photoluminescence. The origin of the ML is discussed and related to the persistent luminescence of BaSi₂O₂N₂:Eu. The same traps are responsible for both the phenomena. Based on the occurrence of ML in this phosphor, we were able to derive that the predominant crystallographic structure of BaSi₂O₂N₂:Eu belongs to space group Cmc2₁.

Keywords

Mechanoluminescence

Luminescence, 358

Photoluminescence, 955, 5775

Phosphor, 358

Piezoelectricity, 642, 1577, 1868, 1991, 2744, 3810

1. Introduction

Mechanoluminescence (ML) is the light emission from materials due to an applied mechanical stimulation. Depending on the type of mechanical action stimulating the emission, ML phenomena are given specific names; *Fractoluminescence* is used when the emitted light is generated through the breaking of chemical bonds by fracture of the material. This has been observed in various organic and inorganic compounds such as sugars, molecular crystals, alkali halides, quartz and minerals [1-4]. *Triboluminescence* is light emission caused by rubbing a material, but actually the emission is generated because of the breaking of the material upon rubbing. Fractoluminescence and triboluminescence are thus often used as synonyms for this destructive type of ML. *Piezoluminescence* is light emission caused by pressure which results only in elastic deformation and is often referred to as elastico mechanoluminescence. As such, piezoluminescence is a non-destructive and, therefore, repeatable ML phenomenon and finds applications in pressure sensing devices [5]. Piezoluminescence has been observed in different classes of compounds such as colored alkali halide crystals, II-VI semiconductors,

quartz and some polymers, but the most efficient ML materials reported are persistent luminescent materials [6-13].

Persistent luminescent materials are phosphors which are able to emit light for a long time after being excited [14]. This remarkable 'afterglow' of persistent luminescence originates in energy storage in the phosphor by trapping of charge carriers in long-lived energy levels inside the band gap. This stored energy can then be released by emission of light after thermal de-trapping of the charge carriers. Many details concerning persistent luminescence, such as the origin of the traps or the transfer pathway from the traps to the luminescent centers remain unclear [14].

Nowadays, the suggested mechanism for piezoluminescence is based on the same principles as persistent luminescence; energy stored in the material is released by light emission after de-trapping of charge carriers. The de-trapping in piezoluminescence, however, is induced by the pressure applied on the material. According to the piezoelectrically induced de-trapping model for piezoluminescence, proposed by Chandra et al. [15, 16], the applied pressure produces a piezoelectric field in the material which can reduce the trap depth or cause band bending. In the case of a decrease in trap depth, de-trapping of trapped charge carriers can occur because of the lower energy barrier. In the case of band bending, charge carriers may tunnel out of their trap levels.

In this paper we report on the strong non-destructive mechanoluminescent (or piezoluminescent) properties of $\text{BaSi}_2\text{O}_2\text{N}_2:\text{Eu}$. This blue-green emitting phosphor is a member of the family of europium doped oxynitrides $\text{MSi}_2\text{O}_2\text{N}_2:\text{Eu}$ (with $\text{M} = \text{Ba}, \text{Sr}, \text{Ca}$),

whose luminescence properties have been described in detail by Bachmann et al. [17]. These europium doped oxynitrides have been proposed as excellent conversion phosphors for white-light-emitting LED applications based on near ultraviolet (UV) to blue emitting InGaN LEDs [18]. Persistent luminescence in europium doped $\text{MSi}_2\text{O}_2\text{N}_2$ (with M = Ba, Sr, Ca) has been reported recently [19]. In brief, after exposure to UV light ($\lambda_{\text{exc}} = 280 \text{ nm}$), all three studied phosphors show afterglow emission, although the emission from $\text{CaSi}_2\text{O}_2\text{N}_2:\text{Eu}$ is very weak. The afterglow intensity of $\text{SrSi}_2\text{O}_2\text{N}_2:\text{Eu}$ and $\text{BaSi}_2\text{O}_2\text{N}_2:\text{Eu}$ is comparable under these excitation conditions. For excitation with near-UV to blue light, the afterglow of $\text{BaSi}_2\text{O}_2\text{N}_2:\text{Eu}$ is two orders of magnitude stronger than $\text{SrSi}_2\text{O}_2\text{N}_2:\text{Eu}$. As $\text{CaSi}_2\text{O}_2\text{N}_2:\text{Eu}$ shows no ML and $\text{SrSi}_2\text{O}_2\text{N}_2:\text{Eu}$ shows only weak ML, we focus in this work on the observed ML in $\text{BaSi}_2\text{O}_2\text{N}_2:\text{Eu}$ and its relation to the persistent luminescence properties.

2. Experimental

$\text{BaSi}_2\text{O}_2\text{N}_2:\text{Eu}$ powders were synthesized using a high temperature solid state reaction. Stoichiometric amounts of starting materials BaCO_3 (99.95%, Alfa Aesar) and Si_3N_4 (α -phase, 99.5%, Alfa Aesar) were weighed and thoroughly mixed in a mortar. In order to dope with Eu, appropriate amounts of BaCO_3 were substituted by EuF_3 (99.5%, Alfa Aesar). The powders were prepared with 2 mol% of Eu. The obtained mixtures were put in zirconia crucibles and fired at 1425°C during 4 hours in a horizontal tube furnace under a flowing atmosphere of forming gas (90% N_2 , 10% H_2). Since the europium ions are incorporated in divalent lattice sites, and the reaction atmosphere is reducing, europium

is predominantly incorporated into the host lattice as Eu^{2+} . After cooling in a natural way, the powders were recuperated from the crucibles and ground in a mortar. $\text{CaSi}_2\text{O}_2\text{N}_2:\text{Eu}$ and $\text{SrSi}_2\text{O}_2\text{N}_2:\text{Eu}$ can be synthesized using the same approach [19].

The crystal structure of the prepared powders was checked by θ -2 θ X-ray diffraction (XRD) measurements (Siemens D5000, $\text{CuK}\alpha$ radiation) and compared with literature data [20]. XRD spectra of the $\text{BaSi}_2\text{O}_2\text{N}_2:\text{Eu}$ powders showed the structure of the $\text{BaSi}_2\text{O}_2\text{N}_2$ host lattice, as reported before [19]. Substituting a small amount of Ba atoms by Eu atoms in the crystal lattice does not have a detectable influence on the XRD spectra and thus we assume that for low doping concentration the crystal structure is unaltered.

To evaluate the ML properties of $\text{BaSi}_2\text{O}_2\text{N}_2:\text{Eu}$, powders were mixed in a transparent epoxy (EPOFIX, Struers GmbH) to form cylindrical samples with a diameter of 2 cm and a thickness of 1 cm. The epoxy is used as a matrix to transmit stress to the $\text{BaSi}_2\text{O}_2\text{N}_2:\text{Eu}$ powder grains. In this way ML samples were prepared with a powder-to-epoxy mass ratio of 1:20, 1:10, 1:5 and 1:3. After optical excitation for about 30 s, compressive strain was applied to the samples while measuring the light emitted by the samples. A 6 watt blacklight (Sylvania F6W/BLB) with an emission maximum at 354 nm and FWHM of 44 nm, positioned at a distance of 20 cm from the sample, was used to optically charge the ML samples. A spectrometer (Ocean Optics QE65000) equipped with an optical fiber was used to record the spectral distribution and the intensity of the mechanoluminescence emitted by the samples. For more accurate measurements, a calibrated photometer (International Light Technologies ILT1700) was used. Tensile tests were performed on a servo-hydraulic

INSTRON 8801 tensile testing machine with a FastTrack 8800 digital controller and a load cell of ± 100 kN. All experiments were done in load-control. For the registration of the compressive data, a combination of a National Instruments 6251 data acquisition card for USB and the SCB-68 pin shielded connector was used. Load, displacement and strain, given by the FastTrack controller, were all sampled on the same time basis.

3. Results

To detect possible ML in the studied phosphors, the following approach was used. A thin layer of phosphor powder is deposited on a substrate, held in place with transparent scotch tape and illuminated by a UV light source. After switching off the light source, the scotch tape is gently rubbed with a pointed object such as a pencil. For $\text{BaSi}_2\text{O}_2\text{N}_2:\text{Eu}$ and $\text{SrSi}_2\text{O}_2\text{N}_2:\text{Eu}$, but not for $\text{CaSi}_2\text{O}_2\text{N}_2:\text{Eu}$, light emission is visible where the pointed object touches the scotch tape. For $\text{BaSi}_2\text{O}_2\text{N}_2:\text{Eu}$ this light emission is intense while for $\text{SrSi}_2\text{O}_2\text{N}_2:\text{Eu}$ this is only weak. A clear afterglow is also visible where the ML originated. In this way, words written with a pointed object on a layer of $\text{BaSi}_2\text{O}_2\text{N}_2:\text{Eu}$ powder remain visible for several seconds (inset of Fig. 1).

To quantify the ML behavior of $\text{BaSi}_2\text{O}_2\text{N}_2:\text{Eu}$, samples were prepared by mixing $\text{BaSi}_2\text{O}_2\text{N}_2:\text{Eu}$ powder in a transparent epoxy (as described above). About 15 s after irradiating the samples using the above mentioned 354 nm UV light source, mechanical stress (in the form of a constant load) is applied for about 35 s on the samples while recording the light emission. Quite similar to the reported ML of Eu, Dy codoped strontium aluminates [21], the samples emit an intense green light when a force is applied

and this light emission attenuates during the time the force is kept constant. When the force is released, the samples produce ML emission again but with much lower intensity (Fig. 1). All of the prepared ML samples with different powder-to-epoxy mass ratios 1:20, 1:10, 1:5 and 1:3 show a similar ML behavior, but the higher the powder-to-epoxy mass ratio, the higher the ML intensity. Application of mechanical stimulation after the sample was kept in the dark for several hours after irradiation, still leads to ML emission albeit with lower intensity. $\text{BaSi}_2\text{O}_2\text{N}_2:\text{Eu}$ not only shows ML emission after excitation with UV irradiation, but also after excitation with blue light with wavelengths up to 480 nm.

Fig. 2 shows the measured photoluminescence (PL) emission spectrum and the ML emission spectrum of $\text{BaSi}_2\text{O}_2\text{N}_2:\text{Eu}$ at room temperature. Both spectra were recorded during the same ML experiment described above. The PL emission spectrum, recorded at an excitation wavelength of 354 nm, peaks around 494 nm and has a FWHM of 32 nm (characteristic for Eu^{2+} emission at this wavelength), this is in good correspondence with literature data [17, 19]. The ML emission spectrum is nearly identical to the PL emission spectrum except for a small shift of about 4 nm towards longer wavelengths. This shift is also observed in the persistent luminescence spectrum, as will be discussed later.

The ML curve from periodically stress-stimulated $\text{BaSi}_2\text{O}_2\text{N}_2:\text{Eu}$ is shown in Fig. 3, together with the applied force profile (a ¼ Hz square wave with a height of 20 kN, corresponding to a pressure of 64 MPa). Again, the sample emitted bluish-green light every time the force was applied. During the time the force was kept constant, the light emission attenuated. When the force on the sample was released, also the ML intensity dropped

very fast. The ML intensity decreases with the number of applied stress stimulations, but after irradiating the sample with UV light the ML intensity recovers completely, indicating that the ML process is non-destructive.

Next, a series of ML experiments were performed using a sensitive photometer (International Light Technologies ILT1700) to quantify the pressure-induced light output and relate it to the afterglow intensity profile. The first experiments were executed as follows: A powder-in-epoxy sample (with 1:10 powder to epoxy ratio) is irradiated for two minutes by 354 nm UV light and the afterglow intensity is measured as soon as the irradiation ends. A certain time after the UV irradiation ended, a constant load is applied on the sample for a specified amount of time while the afterglow intensity is still being measured. The results of these experiments are shown in Fig. 4. Curve (a) shows the regular afterglow, i.e. the afterglow intensity of the unloaded sample as a function of time. Curve (b) shows the afterglow intensity for the experiment where a constant load is applied after one minute until the end of the experiment. As soon as the constant load is applied the afterglow intensity increases instantaneously, then decreases quickly to end up in a regime where the afterglow decays at the same pace as the regular afterglow but at lower intensity. Curve (d) shows a similar experiment except that the constant load is applied after about 70 min. Again, the afterglow follows curve (a) until the load is applied, then shows a sudden increase in intensity followed by a quick decay. Finally, the curves (b) and (d) coincide and decay with the same pace and intensity. Curve (c) corresponds to an experiment in which a constant load is applied on the sample after about 63 s for a period

of 60 s. During the period the load is applied, curve (c) is similar to curve (b) and thus shows the same increase in intensity followed by a fast decay. When the load is removed from the sample, a small increase in intensity is followed by a significant drop in intensity. After some time, the afterglow decays with the same pace as the unloaded sample, being considerably slower than the decay observed during the application of the load. A second series of experiments that were performed is shown in Fig. 5. Again the powder-in-epoxy sample is irradiated for two minutes by 354 nm UV light and the afterglow intensity is monitored as soon as the excitation ends. Then, a constant load is applied on the sample after 3, 5 or 10 min for a short period of 4 s (curves (f), (g) and (h) respectively). All curves in Fig. 5 show the same behavior; the afterglow intensity coincides with the curve of the regular afterglow up till the moment the load is applied, then a huge increase in afterglow intensity is observed. Upon release of the load after 4 s, a sudden decrease in afterglow intensity is observed, however, the afterglow remains above the intensity level of the regular afterglow for some time, after which it drops slowly below the regular afterglow curve. This behavior is in agreement with the observed afterglow after writing on a layer of $\text{BaSi}_2\text{O}_2\text{N}_2:\text{Eu}$ (inset of Fig. 1).

From these experiments, we learn that an abrupt change of the load on the sample (unloaded to loaded state and loaded to unloaded state) results in an instantaneous and abrupt change in afterglow intensity. In loaded condition, the afterglow initially decays faster compared to the regular afterglow and then decays at the same pace as the regular afterglow. Integrating the intensities for the different curves in Fig. 4 during the first

100000 s of the afterglow gives four similar results. The total light emission from the sample is thus independent of the load conditions. Nevertheless, the traps are emptied more quickly by applying a load.

4. Discussion

We observed strong mechanoluminescence (ML) or piezoluminescence for BaSi₂O₂N₂:Eu upon non-destructive application of stress. As shown in Fig. 2, a red-shift of 4 nm can be noticed for the ML emission spectrum, compared to the steady state PL emission spectrum. This shift is not an instrument induced (thus artificial) effect, as both types of emission spectra were recorded on the same apparatus, using identical conditions. Taking the experimental conditions into account (an applied load of 20 kN, corresponding to a pressure of 64 MPa), this shift corresponds to about -2000 cm⁻¹/GPa, which is much larger than what is commonly observed for pressure induced shifts in Eu²⁺ doped compounds, e.g. from -22 cm⁻¹/GPa (β-SiAlON:Eu) to -520 cm⁻¹/GPa (EuCl₂) [22, 23]. To find out whether the shift of the ML emission spectrum depends on the applied force, experiments were performed at different load conditions (12 kN, 16 kN and 20 kN). It turns out that the shift remains the same (± 4 nm) and is thus stress independent. Remarkably, the same shift is also noticed during the persistent luminescence (without applied stress) [19] and the afterglow of the ML. From this, we conclude that the origin of the ML emission in BaSi₂O₂N₂:Eu is presumably the same as that of the persistent luminescence; namely the release of energy, stored in the material, by emission of light after de-trapping of trapped charge carriers.

Given that ML emission can be generated long after the excitation, the traps related to the ML should be at least as deep as the traps emptied during the normal afterglow. However, applying pressure does not lead to an increase in the integrated light output, compared to the afterglow of undisturbed samples (Fig. 4). The traps emptied due to the applied pressure are thus also involved in the persistent luminescence process. From thermoluminescence (TL) measurements in previously published work [19] we observed a TL glow peak at 88°C. The width of the TL glow peak, however, indicates that a trap depth distribution is responsible for this peak, rather than a single trap depth. This is also observed when measuring the TL glow curve with a delay (Fig. 6); the TL glow peak shifts to higher temperatures for longer delay times because the traps with a lower trap depth are emptied faster during the afterglow than those with a slightly deeper trap depth. Multiple traps with only a small difference in trap depth are thus involved in the persistent luminescence process. Hence we can state that the traps related to the ML belong to this same trap depth distribution responsible for the persistent luminescence in BaSi₂O₂N₂:Eu, but that they are emptied faster than in the case of the persistent luminescence, due to the application of mechanical stimulation.

Based on the experimental results, we can propose an energy level scheme for the persistent luminescence and ML in BaSi₂O₂N₂:Eu, situating the important trap levels and Eu²⁺ energy levels inside the band gap of the material (Fig. 7). Upon absorption of UV or blue light by Eu²⁺ ions, the electronic configuration of Eu²⁺ changes from 4f⁷ to 4f⁶5d after which the electron can return to the ground state (i.e. the fast photoluminescence

process) or escape to the conduction band after which trapping at defect levels can occur. In the latter case, an ionized (or trivalent) europium ion is left behind, as was recently shown in the case of the persistent $\text{SrAl}_2\text{O}_4:\text{Eu,Dy}$ phosphor [24]. Based on the TL results discussed above, we can simplify the trap depth distribution by two traps, A and B, being on the shallow and deep edges of the trap distribution. Both traps are involved in the persistent luminescence process: they are emptied thermally, and the electrons released in this way can reach ionized europium ions (through the conduction band) to form excited Eu^{2+} ions in $4f^65d$ state (arrows 1 and 3). De-excitation of the Eu^{2+} ions from $4f^65d$ to the $4f^7$ ground state through emission of light causes the observed afterglow (arrow 2). Trap B is slightly deeper than trap A and is thus emptied more slowly. Upon mechanical stimulation, however, trap B is emptied much faster and the electrons are transferred through the conduction band to the ionized europium ions (arrow 4), after which ML emission is visible (arrow 2). If the electrons, released from trap B upon mechanical stimulation, are re-trapped in trap A before they reach an europium ion (arrow 5 and 6), the occupancy of trap A is increased due to the mechanical stimulation. After the mechanical stimulation is ended, the direct transfer of electrons from trap B to ionized europium ions (arrow 4) stops, causing a sudden drop in ML emission (as observed in Fig. 3, Fig. 4 and Fig. 5), but an increased afterglow related to the thermal release of electrons from the re-populated trap A is visible (as observed in Fig. 5). This energy level scheme is able to explain all observed ML properties of $\text{BaSi}_2\text{O}_2\text{N}_2:\text{Eu}$ powder imbedded in an epoxy

resin and the ML afterglow when 'writing' on a layer of BaSi₂O₂N₂:Eu (inset of Fig. 1) or when applying a short load (inset of Fig. 5) .

To release electrons from trap B (Fig. 7), the mechanical stimulation somehow has to reduce the depth of the trap, or has to provide an extra amount of energy which helps to overcome the thermal barrier associated with the trapped charges. The most recent model for ML emission, the *piezoelectrically induced de-trapping model for piezoluminescence* [15, 16], ascribes the faster release of the trapped charges from trap B to the piezoelectric effect: (i) the application of pressure produces a piezoelectric field, which can be high near defects and activator ions, (ii) the piezoelectric field either lowers the depth of trap B or causes band bending, (iii) the decrease of trap-depth implies that less energy is needed to release the trapped electrons and causes a faster transfer of electrons from trap B to ionized europium ions (arrow 4 in Fig. 7) to form excited Eu²⁺ ions in 4f⁶5d state, while band bending might cause direct tunneling from trap B to the Eu²⁺ 4f⁶5d states or to trap A (arrow 6 in Fig.7), (iv) the de-excitation of the created Eu²⁺ ions from 4f⁶5d to the 4f⁷ ground state through emission of light causes an increase in afterglow, along with a faster decay, as observed for BaSi₂O₂N₂:Eu.

In the piezoelectrically induced de-trapping model for piezoluminescence, a prerequisite for a phosphor to have ML properties is a piezoelectric host material. This has already been shown for europium doped strontium aluminates, as only in its piezoelectric form it is mechanoluminescent [25]. Of the thirty-two crystal classes, twenty exhibit direct piezoelectricity [26]. These classes are: 1, 2, *m*, 222, *mm*2, 4, $\bar{4}$, 422, *4mm*, $\bar{4}2m$, 3, 32,

$3m$, 6 , $\bar{6}$, 622 , $6mm$, $\bar{6}2m$, 23 , $\bar{4}3m$ (Hermann–Mauguin notation for corresponding point groups).

The crystal structure of $\text{BaSi}_2\text{O}_2\text{N}_2$ has been investigated in detail by Kechele et al. [20].

The structure is a stacking of highly condensed silicate layers alternating with layers of Ba^{2+} ions and contains only one Ba site with a rather highly symmetric environment. Based on electron diffraction measurements it was found that $\text{BaSi}_2\text{O}_2\text{N}_2$ crystallizes in an orthorhombic crystal system with lattice parameters $a = 14.44 \text{ \AA}$, $b = 5.34 \text{ \AA}$ and $c = 4.83 \text{ \AA}$. Space group determination based on combined results from electron diffraction, x-ray and neutron powder diffraction and lattice energy calculations led to three possible model structures in space groups Cmcm (no. 63), $\text{Cmc}2_1$ (no. 36) and Pbcn (no. 60). The only difference between these models is a different stacking sequence of the silicate layers, resulting in an ordered stacking for Pbcn and a disordered stacking for both Cmcm and $\text{Cmc}2_1$. As Rietveld refinement data from x-ray and neutron powder diffraction experiments slightly favoured the Pbcn polytype, Kechele et al. proposed this space group for the structure of $\text{BaSi}_2\text{O}_2\text{N}_2$. Nevertheless, many electron diffraction patterns indicated stacking disorder in the structure of $\text{BaSi}_2\text{O}_2\text{N}_2$ and lattice energy calculations for the $\text{Cmc}2_1$ model yielded a slightly better result. Kechele et al. assumed $\text{BaSi}_2\text{O}_2\text{N}_2$ has the tendency to form domains of both structures (in space groups Pbcn and $\text{Cmc}2_1$) with an average structure corresponding to the structure model in Cmcm .

For the possible space groups of the crystal structure of $\text{BaSi}_2\text{O}_2\text{N}_2$ suggested by Kechele et al. only $\text{Cmc}2_1$ (no. 36) belongs to one of the twenty piezoelectric classes ($mm2$). From

the results of Kechele et al. and the strong ML of $\text{BaSi}_2\text{O}_2\text{N}_2$ we thus conclude that $\text{BaSi}_2\text{O}_2\text{N}_2$ has an orthorhombic crystal structure in space group $\text{Cmc}2_1$ or at least contains a significant fraction of domains of this structure. Due to the slightly smaller ionic radius of Eu^{2+} compared to Ba^{2+} , one could argue that the incorporation of Eu ions might distort the lattice structure of $\text{BaSi}_2\text{O}_2\text{N}_2$. Given that the ML emission is also observed for very low dopant concentrations (0.25 mol%), this seems unlikely.

Trap filling in persistent luminescent materials is wavelength dependent and the trap filling spectrum, showing which excitation wavelengths are able to induce persistent luminescence, is often different from the steady state photoluminescence excitation spectrum [27]. For $\text{BaSi}_2\text{O}_2\text{N}_2:\text{Eu}$ trap filling is most efficient by using UV radiation ($\lambda < 325 \text{ nm}$). The traps in the material can also be filled upon excitation with near UV to blue light ($360 \text{ nm} < \lambda < 480 \text{ nm}$), i.e. when exciting into the lowest 5d excited states of Eu^{2+} [19]. This is in good agreement with the fact that ML emission of $\text{BaSi}_2\text{O}_2\text{N}_2:\text{Eu}$ can both be observed after excitation with UV light and after excitation with blue light. For practical applications this is an important aspect, as this reduces the optical requirements of for instance the binding material and allows the use of ambient light or daylight to fill the traps.

Apart from the strong ML emission in $\text{BaSi}_2\text{O}_2\text{N}_2:\text{Eu}$, we observed no ML emission in $\text{CaSi}_2\text{O}_2\text{N}_2:\text{Eu}$ and only a weak ML emission in $\text{SrSi}_2\text{O}_2\text{N}_2:\text{Eu}$. The crystal structure of $\text{SrSi}_2\text{O}_2\text{N}_2$ and $\text{CaSi}_2\text{O}_2\text{N}_2$ is triclinic with space group $\text{P}1$ (no. 1) [28] and monoclinic with space group $\text{P}2_1$ (no. 4) [29] respectively, and thus both belong to a piezoelectric crystal

class (1 and 2 respectively). As $\text{SrSi}_2\text{O}_2\text{N}_2:\text{Eu}$ shows persistent luminescence upon excitation with UV light [19] and its crystal structure is piezoelectric, the observed (weak) ML can be explained using the piezoelectrically induced de-trapping model for piezoluminescence. For $\text{CaSi}_2\text{O}_2\text{N}_2:\text{Eu}$ no ML was observed, this can be related to the fact that $\text{CaSi}_2\text{O}_2\text{N}_2:\text{Eu}$ hardly shows persistent luminescence compared to $\text{BaSi}_2\text{O}_2\text{N}_2:\text{Eu}$ and $\text{SrSi}_2\text{O}_2\text{N}_2:\text{Eu}$ [19]. For this material, the number of (accessible) traps is apparently very low, as is also observed from thermoluminescence glow curves. Consequently, the number of trapped charges which might be released by applying pressure is too low to lead to appreciable ML emission.

5. Conclusions

$\text{BaSi}_2\text{O}_2\text{N}_2:\text{Eu}$ shows strong mechanoluminescence (or piezoluminescence), as upon mechanical stimulation (friction or pressure) intense emission of light is visible. This ML intensity decreases when repeatedly applying stress, but recovers completely by irradiation with UV or blue light. Compared to the PL emission spectrum, the ML emission spectrum shows a shift of 4 nm to longer wavelengths, which is similar to the shift observed for the afterglow. Therefore the origin of the ML emission is presumably the same as for the persistent luminescence, i.e. the recombination of an ionized europium ion and a previously trapped electron. Combining information from ML experiments, persistent luminescence measurements and TL spectroscopy an energy level scheme, based on two trap levels within a trap depth distribution, is constructed which is able to explain all observed persistent luminescence and ML phenomena in $\text{BaSi}_2\text{O}_2\text{N}_2:\text{Eu}$. Based

on the piezoelectric de-trapping model for piezoluminescence, we know that the crystal structure of $\text{BaSi}_2\text{O}_2\text{N}_2:\text{Eu}$ should be piezoelectric, from which we can conclude that $\text{BaSi}_2\text{O}_2\text{N}_2$ has an orthorhombic crystal structure in space group $\text{Cmc}2_1$ or at least contains a significant fraction of domains of this structure.

Acknowledgments

JB and KVdE are Research Assistants for the BOF-UGent. The authors would like to thank Adrie Bos for assisting in the thermoluminescence measurements and Jolien Delepierre for assisting in ML experiments.

References

- [1] Kawaguchi Y. Fractoluminescence spectra in crystalline quartz. *Jpn J Appl Phys* 1998;37:1892.
- [2] Chandra BP, Zink JI. Triboluminescence and the dynamics of crystal fracture. *Phys Rev B* 1980;21:816.
- [3] Sweeting LM. Triboluminescence with and without Air. *Chem Mater* 2001;13:854.
- [4] Tekalur SA. Triboluminescence in sodium chloride. *Journal of Luminescence* 2010;130:2201.
- [5] Ono D, Xu C-N, Li C, Bu N. Visualization of Internal Defect of a Pipe Using Mechanoluminescent Sensor. *Journal of the Japanese Society for Experimental Mechanics* 2010;10:s152.
- [6] Chandra BP. Mechanoluminescence induced by elastic deformation of coloured alkali halide crystals using pressure steps. *Journal of Luminescence* 2008;128:1217.
- [7] Xu CN, Watanabe T, Akiyama M, Zheng XG. Artificial skin to sense mechanical stress by visible light emission. *Appl Phys Lett* 1999;74:1236.
- [8] Reynolds GT. Piezoluminescence from a ferroelectric polymer and quartz. *Journal of Luminescence* 1997;75:295.
- [9] Xu CN, Watanabe T, Akiyama M, Zheng XG. Direct view of stress distribution in solid by mechanoluminescence. *Appl Phys Lett* 1999;74:2414.

- [10] Zhang L, Xu CN, Yamada H, Bu N. Enhancement of Mechanoluminescence in $\text{CaAl}_2\text{Si}_2\text{O}_7:\text{Eu}^{2+}$ by Partial Sr^{2+} Substitution for Ca^{2+} . *Journal of the Electrochemical Society* 2010;157:J50.
- [11] Zhang JC, Wang XS, Yao X, Xu CN, Yamada H. Strong Elastico-Mechanoluminescence in Diphase $(\text{Ba,Ca})\text{TiO}_3:\text{Pr}^{3+}$ with Self-Assembled Sandwich Architectures. *Journal of the Electrochemical Society* 2010;157:G269.
- [12] Chandra VK, Chandra BP. Suitable materials for elastico mechanoluminescence-based stress sensors. *Opt Mater* 2011;34:194.
- [13] Chandra BP. Mechanoluminescent smart materials and their applications. *Electronic and Catalytic Properties of Advanced Materials* 2011:1.
- [14] Van den Eeckhout K, Smet PF, Poelman D. Persistent luminescence in Eu^{2+} -doped compounds: a review. *Materials* 2010;3:2536.
- [15] Chandra BP. Development of mechanoluminescence technique for impact studies. *Journal of Luminescence* 2011;131:1203.
- [16] Chandra BP, Sonwane VD, Haldar BK, Pandey S. Mechanoluminescence glow curves of rare-earth doped strontium aluminate phosphors. *Opt Mater* 2011;33:444.
- [17] Bachmann V, Ronda C, Oeckler O, Schnick W, Meijerink A. Color point tuning for $(\text{Sr,Ca,Ba})\text{Si}_2\text{O}_7:\text{Eu}^{2+}$ for White Light LEDs. *Chem Mater* 2009;21:316.
- [18] Smet PF, Parmentier AB, Poelman D. Selecting conversion phosphors for white light-emitting diodes. *Journal of the Electrochemical Society* 2011;158:R37.

- [19] Botterman J, Van den Eeckhout K, Bos AJJ, Dorenbos P, Smet PF. Persistent luminescence in $\text{MSi}_2\text{O}_2\text{N}_2\text{:Eu}$ phosphors. *Opt. Mater. Express* 2012;2:341.
- [20] Kechele JA, Oeckler O, Stadler F, Schnick W. Structure elucidation of $\text{BaSi}_2\text{O}_2\text{N}_2$ - A host lattice for rare-earth doped luminescent materials in phosphor-converted (pc)-LEDs. *Solid State Sci* 2009;11:537.
- [21] Akiyama M, Xu CN, Liu Y, Nonaka K, Watanabe T. Influence of Eu, Dy co-doped strontium aluminate composition on mechanoluminescence intensity. *Journal of Luminescence* 2002;97:13.
- [22] Kobayashi T, Sekine T. Effect of residual stress on the photoluminescence spectra of EuCl_2 powder. *Opt Mater* 2010;32:1227.
- [23] Tröster T, Schweizer S, Secu M, Spaeth JM. Luminescence of $\text{BaBr}_2\text{:Eu}^{2+}$ under hydrostatic pressure. *Journal of Luminescence* 2002;99:343.
- [24] Korthout K, Van den Eeckhout K, Botterman J, Nikitenko S, Poelman D, Smet PF. Luminescence and x-ray absorption measurements of persistent $\text{SrAl}_2\text{O}_4\text{:Eu,Dy}$ powders: Evidence for valence state changes. *Phys Rev B* 2011;84:085140.
- [25] Xu CN, Yamada H, Wang XS, Zheng XG. Strong elasticoluminescence from monoclinic-structure SrAl_2O_4 . *Appl Phys Lett* 2004;84:3040.
- [26] Nye JF. *Physical properties of crystals: their representation by tensors and matrices*: Clarendon Press, 1985.

[27] Smet PF, Van den Eeckhout K, Bos AJJ, van der Kolk E, Dorenbos P. Temperature and wavelength dependent trap filling in $M_2Si_5N_8:Eu$ ($M = Ca, Sr, Ba$) persistent phosphors *Journal of Luminescence* 2012;132:682.

[28] Hoppe HA, Stadler F, Oeckler O, Schnick W. $Ca[Si_2O_2N_2]$ - A novel layer silicate. *Angew Chem Int Edit* 2004;43:5540.

[29] Oeckler O, Stadler F, Rosenthal T, Schnick W. Real structure of $SrSi_2O_2N_2$. *Solid State Sci* 2007;9:205.

Figure captions

Fig. 1: Typical mechanoluminescence (ML) behavior of stress-stimulated $BaSi_2O_2N_2:Eu$ during application of a force of 20 kN (64 MPa). The solid line shows the ML intensity (on a linear scale) and the dashed line shows the force profile. Inset: Photograph taken after 'writing' the name LUMILAB on a layer of $BaSi_2O_2N_2:Eu$ powder.

Fig. 2: Photoluminescence (PL, excited at 354 nm) and mechanoluminescence (ML) emission spectra of $BaSi_2O_2N_2:Eu$.

Fig. 3: Mechanoluminescence (ML) of $BaSi_2O_2N_2:Eu$, stimulated by a periodically applied external force of 20 kN (64 MPa). The ML intensity on a linear scale (solid line) follows the $\frac{1}{4}$ Hz square wave profile of the external force (dashed line).

Fig. 4: Afterglow intensity as function of time (log-log scale) for different ML experiments on $BaSi_2O_2N_2:Eu$. **(a)** regular afterglow of the unloaded sample. **(b)** constant load applied

after 60 s until the end of the measurement. **(c)** constant load applied after 63 s for a period of 60 s. **(d)** constant load applied after 70 min until the end of the measurement.

Fig. 5: Afterglow intensity, on a log scale, as function of time for different ML experiments on $\text{BaSi}_2\text{O}_2\text{N}_2:\text{Eu}$. **(e)** regular afterglow of the unloaded sample. **(f)** constant load applied after 3 min for 4 s. **(g)** constant load applied after 5 min for 4 s. **(h)** constant load applied after 10 min for 4 s. inset: detail of curve **(h)**.

Fig. 6: Thermoluminescence (TL) glow curves for $\text{BaSi}_2\text{O}_2\text{N}_2:\text{Eu}$ measured with a delay between the excitation of the phosphor and the start of the TL measurement of 0, 6, 20 and 60 min.

Fig. 7: Energy level scheme for the persistent luminescence and mechanoluminescence in $\text{BaSi}_2\text{O}_2\text{N}_2:\text{Eu}$. The different processes are described in the text.

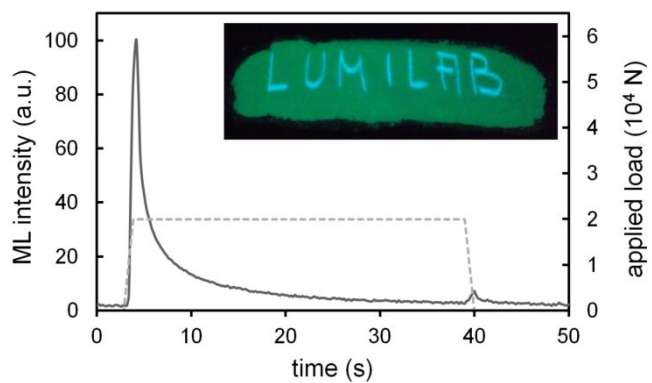


Fig. 1: Typical mechanoluminescence (ML) behavior of stress-stimulated $\text{BaSi}_2\text{O}_2\text{N}_2:\text{Eu}$ during application of a force of 20 kN (64 MPa). The solid line shows the ML intensity (on a linear scale) and the dashed line shows the force profile. Inset: Photograph taken after 'writing' the name LUMILAB on a layer of $\text{BaSi}_2\text{O}_2\text{N}_2:\text{Eu}$ powder.

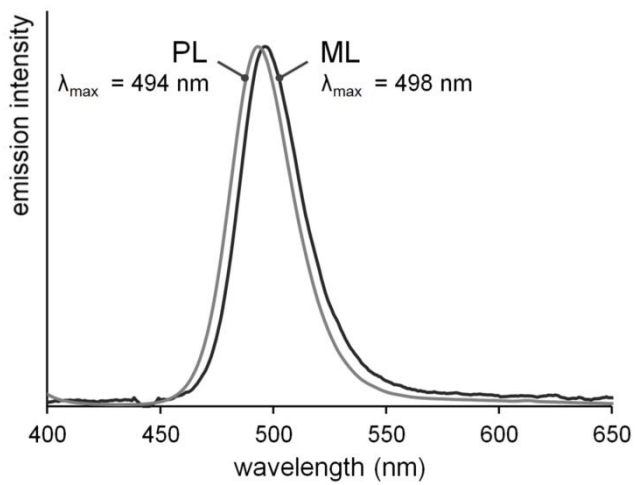


Fig. 2. Photoluminescence (PL, excited at 354 nm) and mechanoluminescence (ML) emission spectra of BaSi₂O₂N₂:Eu.

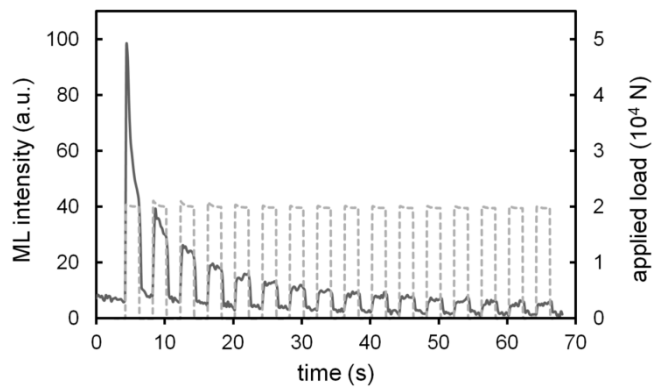


Fig. 3. Mechanoluminescence (ML) of $\text{BaSi}_2\text{O}_2\text{N}_2:\text{Eu}$, stimulated by a periodically applied external force of 20 kN (64 MPa). The ML intensity on a linear scale (solid line) follows the $\frac{1}{4}$ Hz square wave profile of the external force (dashed line).

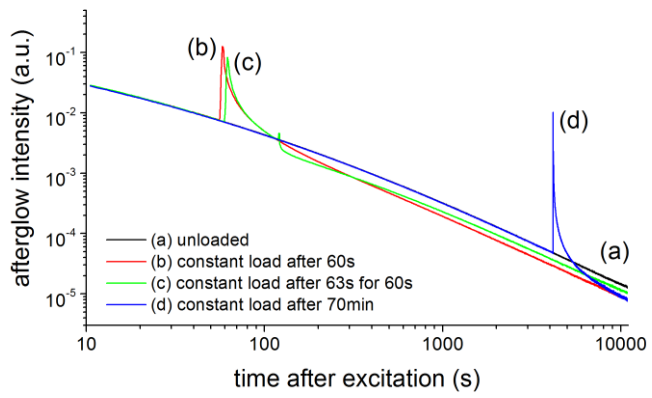


Fig. 4. Afterglow intensity as function of time (log-log scale) for different ML experiments on $\text{BaSi}_2\text{O}_2\text{N}_2:\text{Eu}$. **(a)** regular afterglow of the unloaded sample. **(b)** constant load applied after 60 s until the end of the measurement. **(c)** constant load applied after 63 s for a period of 60 s. **(d)** constant load applied after 70 min until the end of the measurement.

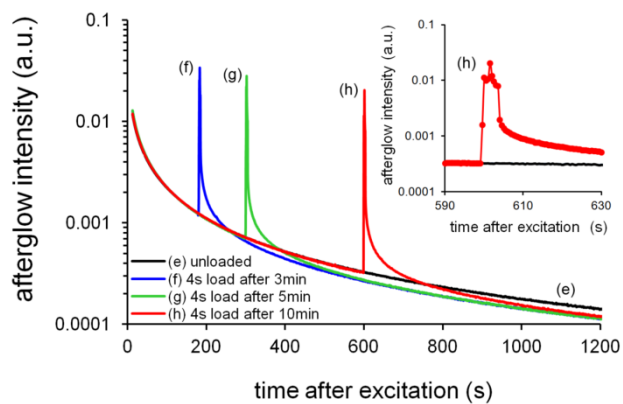


Fig. 5: Afterglow intensity, on a log scale, as function of time for different ML experiments on BaSi₂O₂N₂:Eu. **(e)** regular afterglow of the unloaded sample. **(f)** constant load applied after 3 min for 4 s. **(g)** constant load applied after 5 min for 4 s. **(h)** constant load applied after 10 min for 4 s. inset: detail of curve **(h)**.

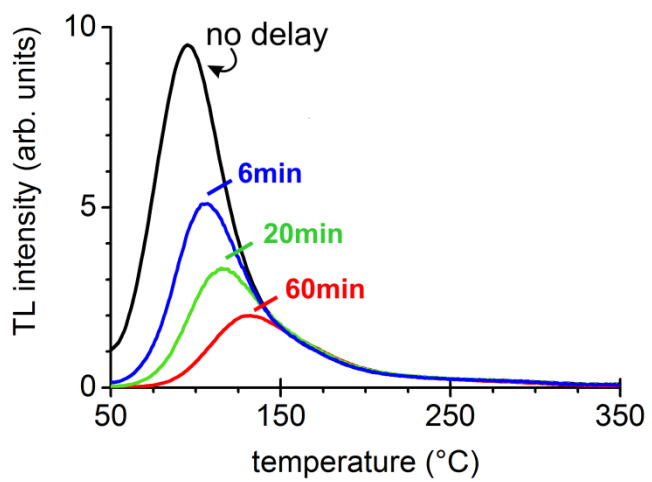


Fig. 6: Thermoluminescence (TL) glow curves for BaSi₂O₂N₂:Eu measured with a delay between the excitation of the phosphor and the start of the TL measurement of 0, 6, 20 and 60 min.

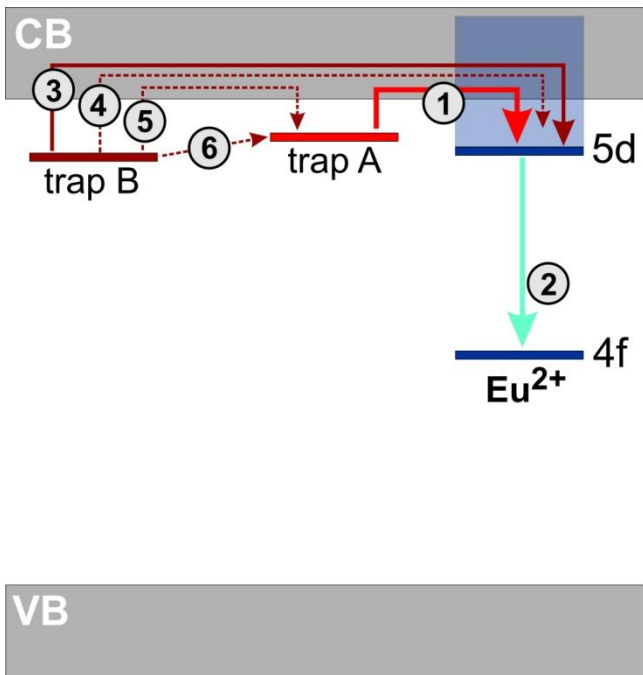


Fig. 7: Energy level scheme for the persistent luminescence and mechanoluminescence in BaSi₂O₂N₂:Eu. The different processes are described in the text.